Development of New Dispersive XAFS Instrument for Time- and Space-Resolved Analysis of Electrode Reactions

Ryota Miyahara, Toshiki Watanabe, Hirona Yamagishi, Misaki Katayama, and Yasuhiro Inada
Department of Applied Chemistry, Graduate School of Life Sciences, Ritsumeikan University, 1-1-1 Noji-Higashi, Kusatsu, Shiga 525-8577, Japan

Abstract

The new instrument based on the dispersive optics for the X-ray absorption fine structure (XAFS) was developed at BL-5 of the SR Center. The vertical axis of the synchrotron radiation is used to disperse the X-ray energy in the newly developed instrument, named vertically dispersive XAFS (VDXAFS) instrument. The vertical energy dispersion is achieved using a cylindrical polychromator, and the horizontal axis of the synchrotron radiation is used to the spatially resolved analysis. The VDXAFS instrument is designed to analyze the dynamic change of the inhomogeneous electrode reaction of secondary batteries during the charge and discharge processes. The line shaped X-ray transmits the electrode sample, and the transmitted X-ray intensities are detected using a two-dimensional detector. The one-dimensional array of XAFS spectra is obtained at the linear footprint of the X-ray on the sample. The VDXAFS system is possible to perform the sequential measurements of the XAFS data array. The time resolution depends on the flux density of the X-ray beam, and the size of the light source affects to the spatial resolution. The latter was estimated to *ca*. 100 μm at BL-5 of the SR Center. The VDXAFS instrument was used to measure the dynamic process of the electrode reaction of $LiFePO_4$ cathode for the charge and discharge processes under the constant current and the charge process under the constant voltage. The obtained results suggest that the reaction distribution depends on not only the electric conductance but also the diffusion process around the reacting particle of $LiFePO_4$.

1. Introduction

Lithium ion secondary battery (LIB) has been widely used for small-scale devices, such as mobile phone and laptop computer, because of its low weight, high energy density and long lifetime. The utilization of LIB has now moved to the electric vehicle for solving the environmental problem by the automobile emission gas. The larger current density and capacity are required for such large-scale purpose. In such cases, the spatially homogeneous progress of the electrode reaction is significantly important, because the inhomogeneous electrochemical reaction causes the unexpectedly large current and the degradation at such specific area.

X-ray absorption fine structure (XAFS) technique has been applied to the *in situ* analysis of various chemical reactions. Because the transmittance of hard X-ray is high and the energies of X-ray absorption edges are characteristics to the element, the XAFS measurements are applicable to samples with the large amount of coexisting materials, such as an outer cell or a solvent. Thus, the synchrotron XAFS technique has been widely applied for the investigations on LIB [1]. Recently, we have reported on the reaction distribution occurring in the $LiFePO_4$ electrode during the charge and discharge processes [2]. The reaction distribution of the electrode in the operating battery was analyzed by using the XAFS imaging technique [3]. The transmittance measurement using a two-dimensional detector enables the spatially resolved XAFS measurement with an element size resolution of the detector. We have concluded that the reaction distribution observed in the $LiFePO_4$ electrode is generated due to the difference of electron conductivity in the electrode. The reaction distribution of $LiFePO_4$ electrode has also been reported with other techniques [4-7]. It has been reported using X-ray diffraction that there are precedent areas such as the area around a collector tab in the porch cell [4] and the side of a separator in the coin-type cell [5]. Ouvrard *et al.* reported the heterogeneous reaction distribution by using the micro-XAFS technique and they hypothesized that the heterogeneity is related to the efficiency of grain connectivity [6]. Wang *et al.* have studied about the dynamic phase transformation process in $LiFePO_4$ at multiple-particle and single-particle scale by using the hard X-ray transmission microscopy [7]. In the study of a multiple-particle of $LiFePO_4$, it has been observed that the phase distribution is homogeneous at the charging rate of 0.1 C and it becomes inhomogeneous at the charging rate of 5 C. Although the various experimental observations show the existence of reaction distributions in the electrode, it is still unclear the detail formation mechanism and the spatial propagation dynamics of the reaction distribution.

Kinetic analysis of a chemical reaction gives information on the reaction mechanism. The time-resolved dispersive XAFS (DXAFS) is the most powerful technique to analyze chemical states of a transition metal species in a real time scale. Matsushita and Phizackerley first reported the concept of the DXAFS technique [8]. The spectrum at a giving energy range is obtained at once without any mechanical motions of the instrument. A white and wide

X-ray beam is irradiated to a cylindrically bent crystal called “polychromator”, and the X-rays diffracted from the polychromator have the different energy in response to the incident angle to the curved crystal surface. The polychromatic X-rays are focused, and a position sensitive detector set behind the focal point measures the dispersed X-ray intensities.

In this study, we have developed a new measurement system based on the DXAFS technique combined with the XAFS imaging technique at BL-5 of the SR Center. It is possible to analyze the time change of the reaction distribution for the LIB electrode using this new instrument. The performance of the developed instrument and its application results about the $LiFePO_4$ positive electrode will be presented in this report. The spatial propagation of the inhomogeneous electrode reaction has been clearly demonstrated during the charge and discharge processes for the $LiFePO_4$ positive electrode.

2. Design of Newly Developed VDXAFS Instrument

The vertically dispersive XAFS (VDXAFS) instrument was constructed at the DXAFS beamline BL-5 of the SR Center. A schematic diagram and a photograph of the VDXAFS instrument are shown in Fig. 1. The rectangular-shaped white X-ray beam is vertically diffracted by a cylindrical polychromator. Because the incident angle of the X-ray to the polychromator crystal changes along the curved surface, the diffracted X-ray energy is dispersed in the vertical direction. The utilization of a two-dimensional detector enables the spatial resolution in the horizontal axis of the incident X-ray beam. The VDXAFS instrument thus makes it possible to analyze the dynamic change of the inhomogeneous electrode reaction of LIBs during the charge and discharge processes.

The incident beam with the size of 4 mm(V) × 10 mm(H) is focused as a line-shape beam, and the electrode sample is placed at the focal position. The transmitted and vertically dispersed X-ray intensities are detected using the CMOS type two-dimensional detector (ORCA-Flash 4.0, Hamamatsu Photonics). The detector has 2048 × 2048 pixels and the element size is 6.5 μm × 6.5 μm. The Tl doped CsI scintillator and 1:1 optical lens system is coupled with the CMOS sensor. The detectable area on the scintillator is 13 mm × 13 mm. The polychromator crystal is placed on the θ stage, and the sample and the detector are installed on the 2θ stage. A weight counter balance is equipped to stabilize the movement of the 2θ axis. A Si(111) crystal with 0.5 mm thickness is used as the cylindrical polychromator, and the crystal is held on a holder which has a fixed concave curvature with the radius of 1 m. The one-dimensional array of XAFS spectra is obtained at the linear footprint of the transmitted X-ray on the sample. The VDXAFS system is possible to perform the sequential measurements of the XAFS data array.

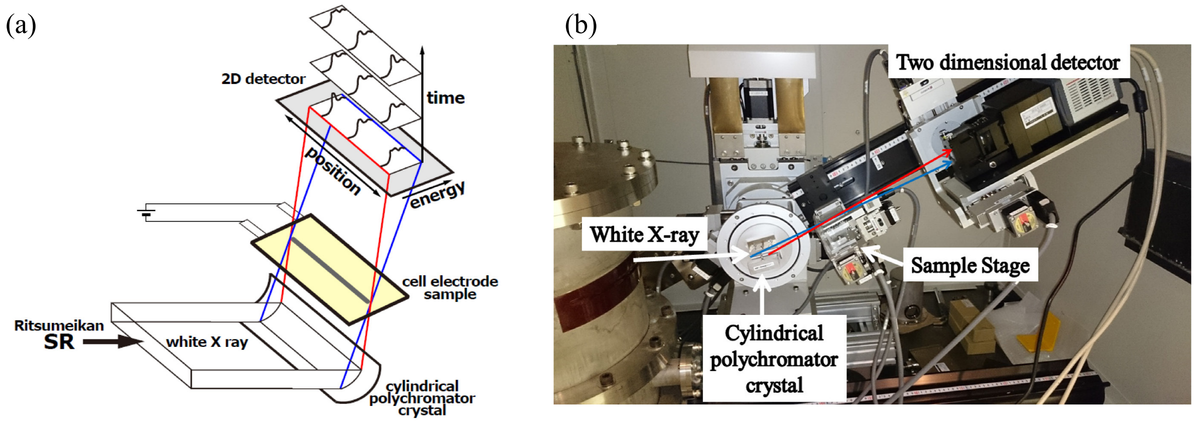

Fig. 1 The schematic diagram (a) and the photograph (b) of the VDXAFS instrument.

3. Performance of VDXAFS Instrument

The VDXAFS measurements were carried out at BL-5 at the vicinity of the Co K edge to evaluate the system performance as the XAFS spectrometer. In Fig. 2, the XAFS spectrum of Co foil measured by the VDXAFS instrument is compared with that obtained using a Si(220) double crystal monochromator at BL-3 of the SR Center. The acquisition time of the VDXAFS measurement was 5 s. The S/N ratio of the obtained spectrum was dependent of the accumulation width in the horizontal direction. The satisfactory quality for the XAFS analysis is achieved by the accumulation width of 100 μm.

The beam divergence in the horizontal direction was estimated by using a slit edge, which is vertically placed at the focal position. Figure 3 shows the horizontal intensity profiles of X rays passed through the slit edge. The distance between the focal point and the detector was changed between 290 and 390 mm. The decreased tailing observed at the close position is explained in considering the size of the light source (1.3 mm(H) × 0.14 mm(V) for the SR Center) and the ratio of the distance between the focal position and the light source to that between the focal position and the detector. The observed profile suggests the horizontal spatial resolution of *ca*. 100 μm at the SR Center. This resolution is strongly related to the size of the light source and thus it is largely improved by using the VDXAFS instrument at the other synchrotron radiation facility with much smaller light source.

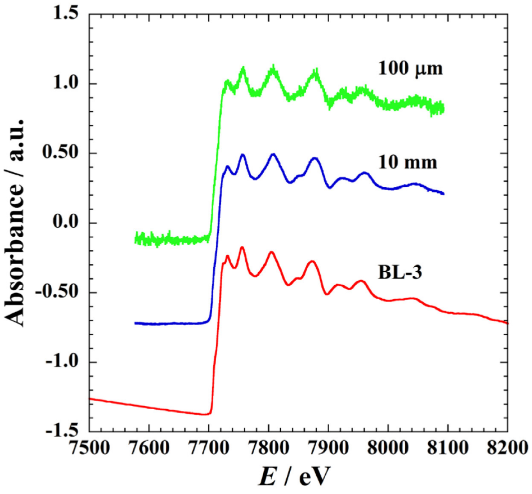

Fig. 2 XANES spectra of Co foil measured using the Si(111) bent crystal with the accumulation width of 100 μm (green) and 10 mm (blue) are compared with that measured using the Si(220) double crystal monochromator (red) at BL-3.

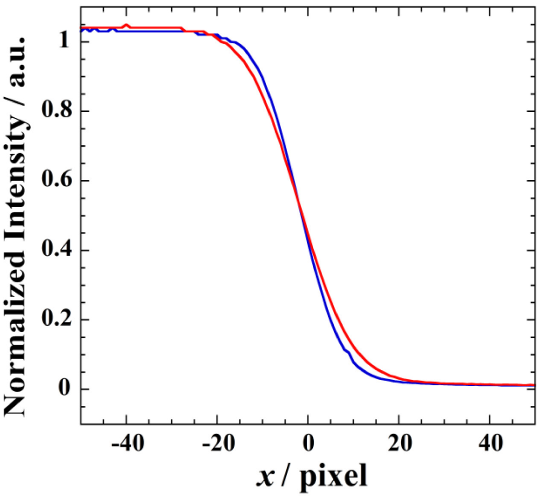

Fig. 3 Horizontal intensity profiles of X-rays passed through a knife edge placed at the focal position. The distance between the focal position and the detector was 290 (blue) and 390 mm (red).

4. Application of VDXAFS to LIB Electrode Reaction

The cathode material was prepared by mixing $LiFePO_4$ powder, acetylene black, and polyvinylidene difluoride with the weight ratio of 75:15:10. The mixture slurry was spread on an aluminum foil with the thickness of 100 μm, and the sheet was dried at 353 K in vacuum for 24 h, and was pressed at 40 MPa for 15 s. A current collector tab was ultrasonically welded to the cathode sheet. The LIB cell was composed of the cathode sheet, a Li foil as the anode, a sheet of polypropylene as the separator, and 1 mol dm^{-3} $LiPF_6$ solution in a 3:7 (v/v) mixture of ethylene carbonate and ethyl methyl carbonate. An aluminum-coated laminate envelope was used as the outer shell of the LIB cell.

The VDXAFS measurements were carried out at BL-5 around the Fe K edge for the charge and discharge processes under a constant current condition of 1 C in the voltage range of 2.0–4.2 V. The dynamic change of the VDXAFS spectra was measured for the charge process of fully discharged LIB under a constant voltage of 4.2 V after the potential jump from 3.1 V. One spectrum was obtained by the accumulation for the width of 300 μm. The exposure time of 5 s was repeated without the interval time for total 4000 s for both processes.

The chemical state of the Fe species was determined by the absorption edge energy, E_0, of the XANES spectrum (Fig. 4(a)). The clear edge shift was observed using the VDXAFS instrument, indicating the reasonable energy resolution of the used cylindrical polychromator. Figure 4(b) and (c) show the results for the charge and discharge processes under a constant current of 1 C. These figures show the time change of the one-dimensional distribution of the chemical state (E_0). Colors in these figures show the chemical state of the Fe species as inserted in Fig. 4(a) and it corresponds to the state of charge. Figure 4(b) shows that the charging reactions at the positions around 0, 3, and 6 mm are precedent in the observed line of the width of 10 mm. It clearly means that the inhomogeneous reaction distribution appears in the observed area, and such positions are regarded to be one of reaction channels, where the electron transfer of the Fe species proceeds in advance. In addition, the observed map for the discharge process given in Fig. 4(c) shows the reverse pattern of the charge process. It means that there are common reaction channels in both charge and discharge processes, because the precedent positions of the electrode reaction are same between the charge and discharge reactions. Such reverse pattern between the charge and discharge processes has previously observed by the XAFS imaging experiment, and it is interpreted that the reaction channels are the electron pathways with the high electronic conductivity [2].

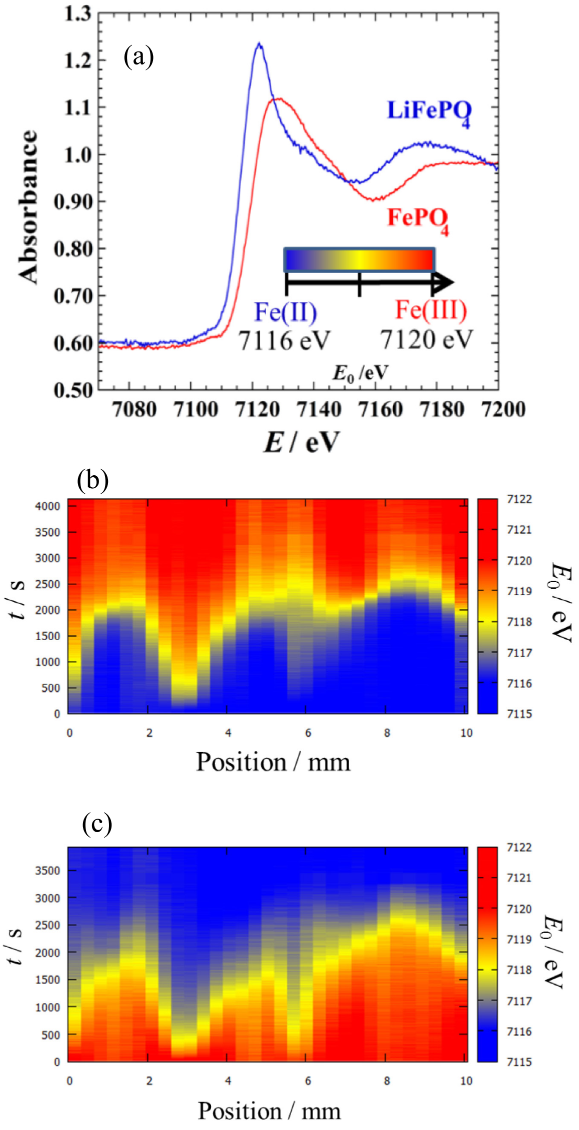

Fig. 4 The accumulated XAFS spectrum (a) and the change of chemical state map of the Fe species as a function of time during the charge (b) and discharge (c) processes.

The time propagation of the reaction distribution after a rapid potential jump was analyzed using the VDXAFS instrument to clarify the elementary processes contributing to the generation of such inhomogeneous electrode reaction. The VDXAFS measurement was carried out at the identical area of Fig. 4, where some reaction channels exist. Figure 5(a) shows the total charging current after the potential jump to 4.2 V applied to the fully discharged cell, and a typical curve of the constant-voltage electrolysis is observed also for the present LIB cell. The E_0 value of the XANES spectrum is given in Fig. 5(b) during the charging process. Because the E_0 value depends on the progress of the electrode reaction, the averaged value for all the measured linear area is shown in Fig. 5(b) as a function of time. The initial large current (> 3.8 mA) vanished within 10 s is assigned to the formation of the electric double layer, because the chemical state of Fe is unchanged at the corresponding time period. The following curves for the current and the E_0 value show very similar feature as seen in Fig. 5, indicating that the average chemical state of Fe for the observed linear area represents the total state of change for the whole cathode electrode.

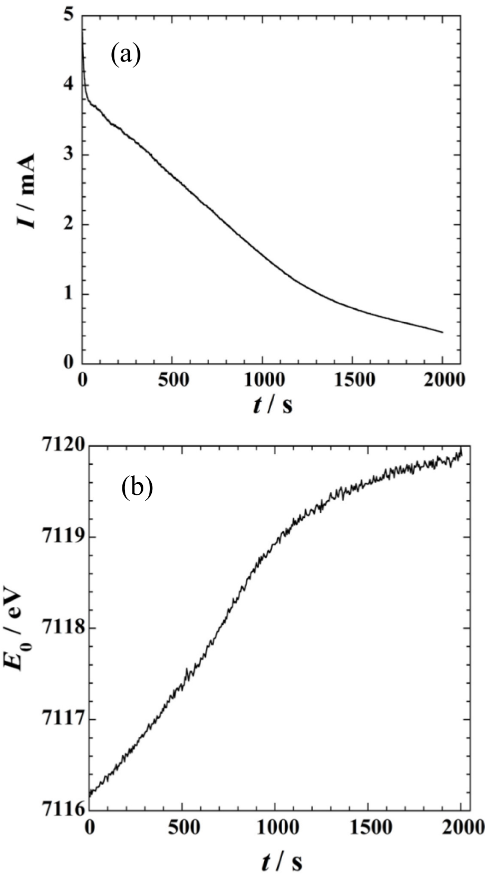

Fig. 5 The change of total electrode current (a) and the average of the absorption edge energy (b) as a function of time after the rapid potential jump at $t = 0$.

The chemical state map during the charging process after a rapid potential jump is shown in Fig. 6(a) as a function of time. The observed pattern seen in Fig. 6(a) is almost consistent with that in Fig. 4(b) for the constant current charging process. The position of the reaction channel is the same for both processes. The change of E_0 at neighboring four positions marked in Fig. 6(a) is shown in Fig. 6(b). The chemical state change at the reaction channel (marked by red circle in Fig. 6(a) and drawn by red line in Fig. 6(b)) seems to be started without any delay time after the potential jump at $t = 0$. The observed time-course curve is satisfactory reproduced by eq. (1),

$$f(t) = A - B\exp(-Ct) + D\sqrt{t} \qquad (1)$$

where A, B, C, and D are the constant values. The exponential term of eq. (1) comes from the first-order charging reaction on $LiFePO_4$ expressed by eq. (2).

$$\mathrm{LiFePO_4} \xrightarrow{k} \mathrm{FePO_4} + \mathrm{Li^+} + \mathrm{e^-} \qquad (2)$$

The early stage of the observed period is predominant by the electron transfer of $LiFePO_4$ accompanied by the Li^+ ion dissociation. The third term of eq. (1) indicates the diffusion process of Li^+ around the reacting particle of $LiFePO_4$, and such process becomes predominant at the late stage of the charging process. It is found that the chemical state change at positions around the reaction channel is initiated after some delay time, and the delay length relates to the distance from the reaction channel. The electrode reaction is started after *ca*. 300 s at the position (marked by yellow square in Fig. 6(a) and drawn by yellow line in Fig. 6(b)) 0.7 mm distant from the reaction channel. The delay time at the position (marked by green diamond in Fig. 6(a) and drawn by green line in Fig. 6(b)) 1 mm distant from the reaction channel is further elongated to *ca*. 500 s. At such positions, the electron transfer process tends to become slow in addition to the delayed start. The larger barrier of the electron transfer process suggests the decreased potential to drive the extraction of electron and Li^+ due to the interrupted electron conductance.

It has been previously concluded that the inhomogeneous reaction distribution is originated with the electron conductivity during the constant current charging and discharging processes [2]. In this study, we have succeeded in observing the distribution propagation by applying the VDXAFS instrument for the charge/discharge processes of the $LiFePO_4$ cathode. The chemical state change of Fe is successively reproduced in considering the electron transfer and the Li^+ diffusion processes. Both processes are fundamental to understand the dynamics of the LIB cathode reaction. The further experiments by changing the composition of the cathode mixture and the concentration of the electrolyte solution will modify eq. (1) to include the delay time as a function of distance from the reaction channel.

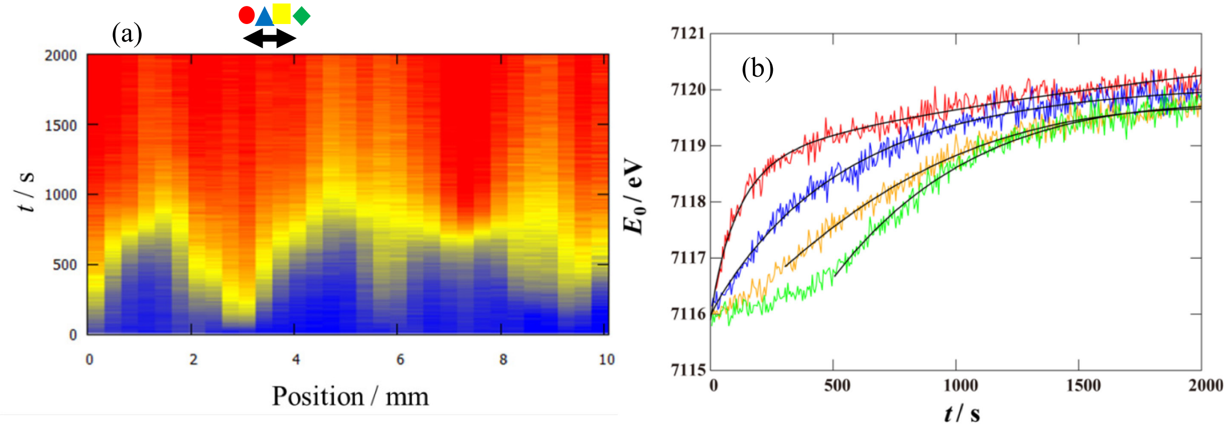

Fig. 6 The chemical state map as a function of time during constant voltage charging process (a) and the time change of the E_0 value at four marked positions (b) after a rapid potential jump to 4.2 V.

5. Conclusion

The originally designed VDXAFS instrument has been developed for the time- and space-resolved XAFS measurements to analyze the inhomogeneous reaction distribution appeared in the $LiFePO_4$ positive electrode of LIB. The spatial resolution of the VDXAFS instrument is *ca*. 100 µm when it is used at the SR Center. The VDXAFS instrument has been applied to observe the propagation of the inhomogeneous distribution of the $LiFePO_4$ electrode. The reaction distribution has been successfully observed in the one-dimensional array of the XAFS spectra for the constant current charge/discharge processes as seen by the two-dimensional XAFS imaging method. A few reaction channels were observed in the observed line with 10 mm width, and the 100-μm scale of spatial inhomogeneity was in agreement with that previously reported. The VDXAFS instrument permitted us to observe the dynamic homogenization process of the inhomogeneous reaction distribution. Similar to the constant current processes, the generation of the inhomogeneous distribution was observed during the dynamic process of the charging reaction after a rapid potential jump. The electrode reaction proceeded in advance at some reaction channels, and the position of the reaction channels was the same as that observed during the constant current processes. The change of the chemical state of Fe as a function of time was reproduced by an equation, in which both the electron transfer process and the Li^+ ion diffusion process were considered. The present results suggest that not only the electronic conductivity but also the diffusion of Li^+ contribute to the generation of the inhomogeneous reaction distribution.

References

[1] I. Nakai, K. Takahashi, Y. Shiraishi, T. Nakagome, F. Izumi, Y. Ishii, F. Nishikawa, and T. Konishi, *J. Power Sources*, **68**, 536-539 (1997).

[2] M. Katayama, K. Sumiwaka, R. Miyahara, H. Yamashige, H. Arai, Y. Uchimoto, T. Ohta, Y. Inada, and Z. Ogumi, *J. Power Sources*, **269**, 994-999 (2014).

[3] M. Katayama, K. Sumiwaka, K. Hayashi, K. Ozutsumi, T. Ohta, and Y. Inada, *J. Synchrotron Rad.*, **19**, 717-721 (2012).

[4] J. Liu, M. Kunz, K. Chen, N. Tamura, and T. J. Richardson, *J. Phys. Chem. Lett.*, **1**. 2120-2123 (2010).

[5] F. C. Strobidge, B. Orvananos, M. Croft, H. C. Yu, R. Robert, H. Liu, Z. Zhong, T. Connolley, M. Drakopoulos, K. Thornton, and C. P. Grey, *Chem. Mater.*, **27**, 2374-2386 (2015).

[6] G. Ouvrard, M. Zerrouki, P. Soudan, B. Lestriez, C. Masquelier, M. Morcrette, S. Hamelet, S. Belin, A. M. Flank, and F. Baudelet, *J. Power Sources*, **229**, 16-21 (2013).

[7] J. Wang, Y. C. Karen, C. Wiegart, and J. Wang, *Nat. Commun.*, **5**, 1-10 (2014).

[8] T. Matsushita and R. P. Phizackerley, *Jpn. J. Appl. Phys.*, **20**, 2223-2228 (1981).